Review of Contemporary Philosophy
ISSN: 1841-5261, e-ISSN: 2471-089X
Vol 22 (1), 2023
pp. 74 – 84

Computer Aided Diagnosis Model for Haemorrhage Detection using Improved Equilibrium Optimization with Deep Learning on CT Images

Mousa Murayshid Hubaylias Almutari[1], Ibrahim M Mehedi[2], Naif Shatwa Saud Alyami[1], Bader Dakhilallah Samran Alrashdi[1], Nadr Saleh Falah Alenzi[1], Mohammed Ali M Alrasheedi[1], Samran Dakhilallah Samran Alrashdi[1], Mahendiran T Vellingiri[3] and Salman Arafath Mohammed[4]

[1]Ministry of Health, Saudi Arabia

2Department of Electrical and Computer Engineering, King Abdulaziz University, Jeddah, Saudi Arabia

[3]Department of Electrical and Computer Engineering, King Abdulaziz University, Jeddah, Saudi Arabia

[4]Department of Electrical Engineering, Computer Engineering Section, College of Engineering, King Khalid University, Abha, Saudi Arabia

Abstract—Intracranial haemorrhage (ICH) recognition is a crucial challenge in neurology and radiology, as on time detection of haemorrhages within brain help in fast involvement and treatment. Numerous image modalities, with magnetic resonance imaging (MRI) and computed tomography (CT) are widely utilized to perceive and categorize ICH. Traditional models for ICH recognition are trusted on physical assessment of CT images by expert radiologists. But, with developments in machine learning (ML), deep learning (DL) and computer aided methods are mainly established to aid radiologists in identifying and detecting ICH professionally. DL methods like convolutional neural networks (CNN) have revealed excellent outcomes in ICH recognition on CT images. This article presents Improved Equilibrium Optimization with Deep Learning for ICH detection (IEODL-ICHD) technique on CT images. The IEODL-ICHD technique starts with the UNet segmentation approach which proficiently outlines the regions of interest for ICH detection. Besides, the IEODL-ICHD technique utilizes the ResNet18 feature extractor to extract high-level features to accurately identify the haemorrhage. Furthermore, the IEO model is exploited for hyperparameter tuning, safeguarding the model's flexibility to the refined features of the ICH. Lastly, the extreme gradient boosting (XGBoost) model is applied for accurate recognition and classification of the ICH. The simulation results of the IEODL-ICHD technique are systematically authenticated on CT images, representing greater performance in ICH classification.

Keywords— Intracranial Haemorrhage; Computed Tomography; Computer Aided Diagnosis; Deep Learning; Equilibrium Optimization

Received:13 May 2023 **Revised:** 02 July 2023 **Accepted:**15 August 2023

1. Introduction

Intracranial haemorrhage (ICH) exposes as a flow inside the intracranial vault. ICH is a neurological disaster that has numerous subtypes like caudate nucleus, basal ganglia, or pons [1]. These haemorrhage are normally based on the anatomical position of bleeding. As per the American Stroke and Heart Association, the initial and timely analysis of ICH is important because it will weaken the affected patients within a few hours after the incident [2]. Non-contrast head computer tomography (CT) is the imaging modality employed to identify haemorrhage owing to its extensive accessibility and velocity [3]. This method has exposed the highest sensitivity and specificity in noticing acute haemorrhage [4]. CT is the most generally utilized medical imaging method to evaluate the violence of brain haemorrhage in traumatic brain injury (TBI). TBI is a very dangerous disease as even a few minutes delay can cause death [5]. Traditional techniques contain visual examination by radiologists and measurable assessment of the

dimensions of hematoma and midline change physically [6]. The whole process is time consuming and needs the accessibility of expert radiologists at every instant. Therefore, automatic hemorrhage recognition tools provide quick inference [7].

Deep learning (DL) based automatic diagnosis techniques have been attracting more interest currently mostly owing to their quicker inference and capability to achieve difficult cognitive tasks or else needed specialized knowledge and experience [8]. In the present scenario, many DL based artificial intelligence (AI) models are effectively proposed for medical imaging analysis tasks with an accuracy corresponding to expert physicians, such as breast cancer recognition, analysis of skin cancer, and the classifying of diabetic retinopathy [9]. The AI models can work as a 2nd reader to guarantee appropriate recognition of high-impact subtle results and can perform as a triage device to simplify the on-time analysis of important events [10]. There previously occurred a few works on the growth of DCNN techniques for the automatic recognition and identification of ICH.

This article presents Improved Equilibrium Optimization with Deep Learning for ICH detection (IEODL-ICHD) technique on CT images. The IEODL-ICHD technique starts with the UNet segmentation approach which proficiently outlines the regions of interest for ICH detection. Besides, the IEODL-ICHD technique utilizes the ResNet18 feature extractor to extract high-level features to accurately identify the haemorrhage. Besides, the IEO model is exploited for hyperparameter tuning, safeguarding the model's flexibility to the refined features of the ICH. Lastly, the extreme gradient boosting (XGBoost) model is applied for accurate recognition and classification of the ICH. The simulation results of the IEODL-ICHD technique are systematically authenticated on CT images, representing greater performance in ICH classification.

I. LITERATURE SURVEY

In [11], an automated method of classifying ICH from a CT scan is developed. To categorize ICH precisely, the offered technique enhanced the Densely Connected Convolutional Network (DenseNet) utilizing the Bayesian Optimizer (BO) model. The study also used BO to describe the finest learning rate, quantity of nodes, and optimizer in the dense layer. Mansour and Aljehane [12] improved the innovative DL-ICH method employing optimum image segmentation with Inception System. At first, an input data endure format change. Then, Kapur's threshold with elephant herd optimizer (EHO) model named KT-EHO was used for image segmentation. Last, the DL based Inceptionv4 system is used as a feature removal, and an MLP is employed for identification. Alfaer et al. [13] develop an automatic ICH analysis utilizing a fusion-based DL with SI (AICH-FDLSI) model. The median filtering (MF) technique is utilized for pre-processing. Then, the seagull optimizer algorithm (SOA) with Otsu multi-level threshold is applied for segmentation. The CapsNet and EfficientNet are functional for feature removal, and the deer hunting optimizer (DHO) procedure was applied for the hyperparameter optimizer. Lastly, a fuzzy SVM (FSVM) can useful as a method of classification.

Ragab et al. [14] concentrate on the growth of a Political Optimizer with DL based ICH Diagnosis on Healthcare Management (PODL-ICHDHM) model. For extraction of feature, the Faster SqueezeNet technique can be applied in this research. Finally, the PO model with the DAE method has been used for the identification of ICH precisely. In [15], a CNN optimizer model dependent on the BAS optimizer procedure is developed. The technique enhances the early parameters of the CNN over the BAS optimizer system. Depending on this optimizer technique, a new CNN method with a pre-trained BAS optimizer model was planned and used to study the medical imaging data for ICH. In [16], an optimum DL framework is projected. Initially, the setup of raw input data can be changed from three-dimensional DICOM to NIfTI. Lastly, a measurable valuation system is accepted to mechanically measure both volume and thickness over the 3-D shape mask joint by the output prospects of the identification system.

2. The Proposed Method

In this article, we have presented a novel IEODL-ICHD technique on CT images. The main purposes of the IEODL-ICHD methodology encompass four different processes namely UNet segmentation, ResNet18 feature extractor, IEO-based parameter tuning, and XGBoost based classification. Fig. 1 depicts the entire flow of IEODL-ICHD technique.

A. UNet segmentation

The IEODL-ICHD technique starts with the UNet segmentation approach which proficiently outlines the regions of interest for ICH detection. UNet is considered an effective model that even works well with fewer training samples in image segmentation based on DL algorithms [17]. The 'U' shaped structure of UNet is balanced and consists of dual main sections namely expanding and contracting network. Using these layers, Up-sampling and Down-sampling of images can be performed. The expanding network is composed of transposed 2D convolution (2DConv) layers while the contracting network is composed of a general convolution process. This model doesn't have any full connection layers. Each of the expanding paths and contracting paths comprises four sections. There is another section of Conv layers in the central to connect these two paths. Each section has three 3×3 padded Conv layers in the contracting path that maintains input dimension. Among them, the central layer has double the number of feature networks than others. After each of the three Conv layers, Batch normalization (BN) and the rectified linear unit ($ReLu$) are included in every section. The 2×2 max-pooling operation is carried out during down-sampling with the stride of 2. The feature channel gets doubled during down-sampling. The transitional section that interconnects the expanding path and the contracting way has a parallel Conv layer. Up-sampling is the basic function of expanding the path and the feature maps get upsampled at each section. This is followed by 2×2 Conv layers to reduce the number of feature networks by half. Next, a concatenation process is carried out among the respective feature map and feature channels from the contracting path. Followed by three padded 3×3 Conv layers, the concatenation operation is performed to maintain the feature channel number that exactly has a similar format to the section in the contracting path. Each 3×3 Conv layer in all sections of the expanding path is followed by BN and ReLU. The 1×1 Conv layer is added for deciding the class for all the feature vectors. The UNet model has an overall of 32 Conv layers. The architecture of UNet has a contracting track to capture a symmetric and context-expanding track for exact localization. In that regard, precise segmentation outcome is even possible with a limited number of training data.

Fig. 1. Overall flow of IEODL-ICHD technique

B. ResNet18 feature extractor

In this work, the IEODL-ICHD technique utilizes the ResNet18 feature extractor to extract high-level features to accurately identify the haemorrhage. Kaiming He et al. 2015 developed ResNet, a novel deep convolution neural network (DCNN) architecture and its underlying concept is to resolve the expression bottleneck and gradient vanishing problems in deep neural networks by introducing "residual block" [18]. The classical deep network has the gradient vanishing problem, and the backpropagated gradient signal becomes weak as the number of network layers increases, resulting in training difficulty. Also, the Residual block allows direct connection across layers, thereby facilitating data transmission:

$$y_l = h(x_l) + F(x_l, W_l)x_{l+1} = f(y_l) \quad (1)$$

Where $(x) = F(x) +$ is the constant mapping function, x is the input, and $F(x)$ is the mapping function G. When $F(x)$ tends to 0, it implies that $G(x) = x$ by constant mapping. The learning feature from shallow l to deep L is attained by Eq. (2):

$$x_L = x_l + \sum_{i=l}^{L-1} F(x_{l^F} W_l) \quad (2)$$

Where x_l and $x_{(l+1)}$ are the input and output of l^{th}residual units, correspondingly, $F()$ refers to the residual function, $h(x_l) = x_l$ indicates the constant mapping, and f shows the ReLu activation function.

C. Hyperparameter tuning using IEO

In this stage, the IEO model is exploited for hyperparameter tuning, safeguarding the model's flexibility to the refined features of the ICH. EO is a nature-inspired and population-based metaheuristics that fits to the type of Physics-based optimizer models inspired by dynamic source and descend methods with a physics basis that are employed to create refined estimates regarding equilibrium conditions [19]. EO randomly prepares the population positions and its position upgrade is determined as:

$$X_i(n+1) = X_{eq}(n) + (X_i(n) - X_{eq}(n))\,F(n) + \frac{G(n)}{\lambda}(1F(n)) \quad (3)$$

whereas X_{eq} defines the equilibrium pool, and it can be generated by the locations of 1st four optimum results and their normal rate. This method arbitrarily selects one from X_{eq} for all the runs. F controls the balance among exploration as well as exploitation, as expressed in Eq. (5).

$$t(n) = (1 - \frac{n}{Max\_iter})^{(2\frac{n}{Max\_iter})} \quad (4)$$

$$F(n) = sign(r - 0.5)[e^{-\lambda t(n)} - 1] \quad (5)$$

In which, Max_iter implies the maximal iteration. λ and r refer to the 2 random numbers from the interval of 0 and 1. $Sign$ denotes the signum function of Matlab. G supports the method in attaining optimum solution, and it can be estimated as.:

$$GCP = \{0.5r1 \;\; if(r2 \geq GP)\; 0 \qquad else \quad (6)$$

$$G_0(n) = GCP * (X_{eq}(n) - X_i(n)) \quad (7)$$

$$G(n) = G_0(n) * F(n) \quad (8)$$

Whereas, $r1$ and $r2$ represent the 2 random values among zero and one.

In EO, performances are led by the equilibrium pool. But, the existence of the 4 optimum performances can be placed at a local optimal and is possibly trapped through the population. Otherwise, if these performances can be scattered in distinct searching regions, it hinders convergence.

Exploitation and exploration are 2 important features utilized for evaluating the efficacy of meta-heuristic techniques. Improved search develops the EO's global search capability and supports escape from

local optimum. Furthermore, optimum exploration enables the method with robust local search capability and encourages it to completely effort potential areas and realize the optimum result. In early the presented BiEO, the people is separated into 3 sub-swarms. The primary sub-swarm concentrates on exploration skills and the secondary sub-swarm preserves population assortment and convergence. The final sub-swarm is in control of exploitation skills, and the sub-swarms segment useful data.

The transfer function (TF) roles a vital play in dual meta-heuristic systems and it can be dependable to convert consistent outcomes into a binary string. An appropriate TF is to assist in maintaining assortment in the population, avoid early convergence, and secure effectual exploration of searching space. It employs 3 TFs and Eq. (9) to execute binarization.

$$X_i^j(n+1) = \{X_i^j(n) \;\; if(S(value) < rand)\; 1 - X_i^j(n) \;\; else \tag{9}$$

$$value = (X_i(n) - X_{eq}(n))\, F(n) + \frac{G(n)}{\lambda}(1 - F(n)) \tag{10}$$

In which, S refers to the TF, and $X_i^j(n)$ signifies the individual position i within the j^{th} dimension at n^{th} iteration.

During the primary sub-swarm, the equilibrium pool has been generated by the sub-swarm, and it implements S_1 as it TF but S_1 rapidly switches locations. This sub-swarm searches bigger places, and it takes great global search capability. During the secondary sub-swarm, it assumes S_2 as its TF. It takes the benefits of EO, and it equilibriums local and global searches. During the tertiary sub-swarm, X_{eq} is created of the global optimum performance, and this sub-swarm accepts S_3 as it TF whereas S_3 gradually alters positions. The sub-swarm acts with optimum performances, and it has outstanding local search capability.

The IEO model originates a fitness function (FF) to get superior classification performance. It defines a positive number to signify the enhanced candidate solution performance. In this research, the error rate of classification minimization is measured as FF and assumed in Eq. (11).

$$fitness(x_i) = ClassifierErrorRate(x_i)$$
$$= \frac{No.of\ misclassified\ instances}{Total\ no.of\ instances} * 100 \tag{11}$$

D. XGBoost based classification

Lastly, the XGBoost model is applied for accurate recognition and classification of the ICH. XGBoost is a robust ML device that is open source. It works by combining gradient boosting and decision trees (DTs) and is estimated to help in the growth of superior methods [20]. Usability, huge dataset performance, and rapidity are significant in XGBoost design. It does not need parameter optimizer or alteration, so, it might be utilized in correct away after installation without extra settings. Utilizing the weighted quantile sketch procedure, XGBoost also can manage sparse datasets. By upholding a similar level of computational difficulty as prior systems such as stochastic gradient descent, this procedure permits us to manage feature matrices that contain nonzero elements. At the time of the computation phase, XGBoost utilizes disk-based data structures to deliver core processing abilities. Therefore, XGBoost is chosen due to its great implementation speed.

The XGBoost function is as follows: Consider the dataset as a DS, which has m features, and n denotes the amount of samples. $DS = \{(x_i, y_i): i = 1 \ldots n, x_i \in R^m, y_i \in R\}$. Consider $\hat{y}$ as the forecast result of an ensemble method formed from Eq. (12).

$$A.i = \emptyset(X_i) = \sum_{k=1}^{K} f_k(X_i), f_k \in l \tag{12}$$

Whereas, K signifies the number of trees, f_k refers to the kth tree. Now, we want to calculate the best function by decreasing the regularization and loss

$$L(\emptyset) = \sum_{i} \quad l(y_i, A \cdot_i) + \sum_{k} \quad \Omega(f_k) \qquad (13)$$

Where l signifies the loss function, y_i and $\hat{y}$ denotes the actual and predicted output, respectively, Ω denotes a complexity measure.

$$\Omega(f_{k}) = \gamma T + \frac{1}{2}\lambda||w||^2 \qquad (14)$$

Over-fitting is calculated utilizing the Eq. (14)

Where T means the amount of trees and w signifies the leaf weight. In DTs, boosting is employed in the training method in order to decrease the function of the objective. So, t^{th} iteration, a novel function has been comprised as presented in Eqs. (15) to (17).

$$L^{(t)} = \sum_{i=1}^{n} \quad l\,(y_{i}, A_{i}^{(t-1)} + f_{t}(x_{i})) + \Omega(f_{t}) \qquad (15)$$

$$-1 \quad (\Sigma_{igl}\ g_i)^2 \qquad (\Sigma_{igl}\ g_i)^2 \qquad (\Sigma_{i\in I9i})^2$$

$$L_{split} \frac{}{2}\left[\frac{L}{\Sigma_{igl_L} h_i + \lambda} + \frac{R}{\Sigma_{isI_R} h_i + \lambda} - \frac{}{\Sigma_{igl} h_i + \lambda}\right] - \gamma \quad (16)$$

$$Where\ L^{(t)} = \sum_{i=1}^{n} \quad l\,(y_{i}, A_{i}^{(t-1)} + f_{t}(x_{i})) + \Omega(f_{t}) \qquad (17)$$

$$and\ h_{i} = \delta^2_{A^{(t-1)}}\ 1(y_{i}, A^{(t-1)}) \qquad (18)$$

3. Results Analysis and Discussion

In this section, the ICH detection performance of the IEODL-ICHD technique is tested using benchmark dataset, containing 341 samples with five classes as demonstrated in Table 1.

Fig. 2 illustrates the confusion matrices produced by the IEODL-ICHD system under 60:40 TRAP/TESP and 70:30 TRAP/TESP. These results indicate the effective recognition with five classes.

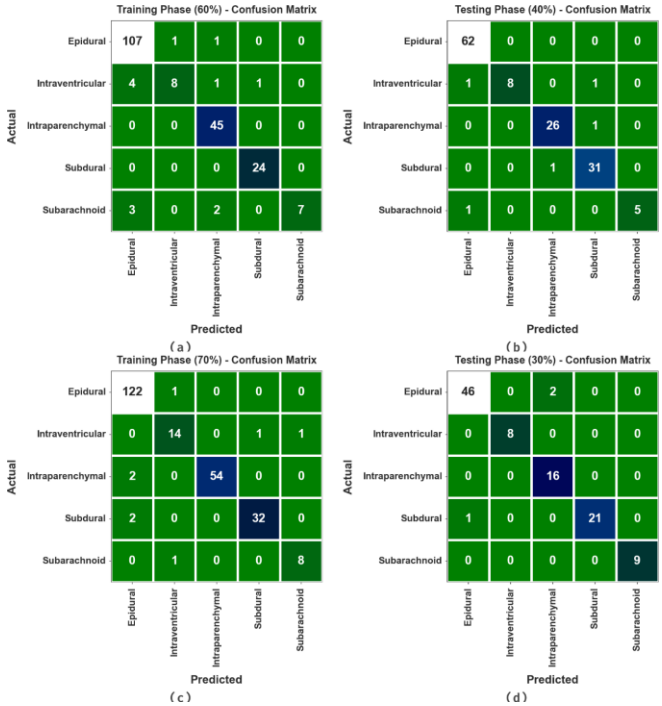

Fig. 2. Confusion matrices of IEODL-ICHD under (a-b) 60:40 TRAP/TESP and (c-d) 70:30 TRAP/TESP

The ICH detection output of the IEODL-ICHD technique is displayed in Table 2 and Fig. 3. These obtained outcomes highlighted the effectual recognition proficiency of the IEODL-ICHD technique. According to 60% of TRAP, the IEODL-ICHD technique gains average $accu_y$, $prec_n$, $reca_l$, F_{score} and MCC of 97.45%, 94.12%, 82.73%, 86.58%, and 85.73%. Also, based on 40% of TESP, the IEODL-ICHD algorithm provides average $accu_y$, $prec_n$, $reca_l$, F_{score} and MCC of 98.54%, 97.42%, 91.30%, 93.98%, and 93.23%, respectively.

Table I Details Of Dataset

Classes	**No. of Instances**
Epidural	171
Intraventricular	24
Intraparenchymal	72
Subdural	56
Subarachnoid	18
Total Instances	**341**

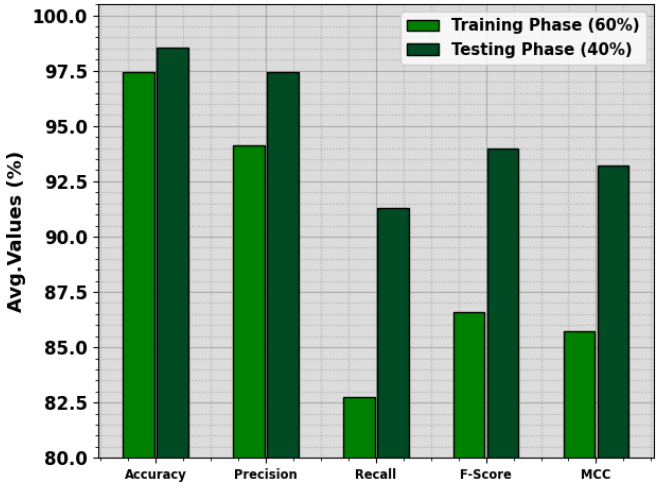

Fig. 3. Average of IEODL-ICHD system under 60:40 TRAP/TESP

The ICH detection output of the IEODL-ICHD system can be determined in Table 3 and Fig. 4. These accomplished outcomes indicated the effective recognition ability of the IEODL-ICHD algorithm. According to 70% of TRAP, the IEODL-ICHD method achieves average $accu_y$, $prec_n$, $reca_l$, F_{score} and MCC of 98.66%, 94.04%, 93.22%, 93.62%, and 92.67%. Similarly, with 30% of TESP, the IEODL-ICHD system obtains average $accu_y$, $prec_n$, $reca_l$, F_{score} and MCC of 98.83%, 97.35%, 98.26%, 97.73%, and 96.89%, correspondingly.

Table Ii Ich Detection Output Of Ieodl-Ichd Method Under 60:40 Trap/Tesp

Classes	$Accu_y$	$Prec_n$	$Reca_l$	F_{score}	***MCC***
TRAP (60%)					
Epidural	95.59	93.86	98.17	95.96	91.22
Intraventricular	96.57	88.89	57.14	69.57	69.70

Intraparenchymal	98.04	91.84	100.00	95.74	94.62
Subdural	99.51	96.00	100.00	97.96	97.71
Subarachnoid	97.55	100.00	58.33	73.68	75.40
Average	**97.45**	**94.12**	**82.73**	**86.58**	**85.73**
TESP (40%)					
Epidural	98.54	96.88	100.00	98.41	97.10
Intraventricular	98.54	100.00	80.00	88.89	88.75
Intraparenchymal	98.54	96.30	96.30	96.30	95.39
Subdural	97.81	93.94	96.88	95.38	93.97
Subarachnoid	99.27	100.00	83.33	90.91	90.94
Average	**98.54**	**97.42**	**91.30**	**93.98**	**93.23**

Table Iii Ich Detection Output Of Ieodl-Ichd Model Under 70:30 Trap/Tesp

Classes	$Accu_y$	$Prec_n$	$Reca_l$	F_{score}	***MCC***
TRAP (70%)					
Epidural	97.90	96.83	99.19	97.99	95.82
Intraventricular	98.32	87.50	87.50	87.50	86.60
Intraparenchymal	99.16	100.00	96.43	98.18	97.66
Subdural	98.74	96.97	94.12	95.52	94.80
Subarachnoid	99.16	88.89	88.89	88.89	88.45
Average	**98.66**	**94.04**	**93.22**	**93.62**	**92.67**
TESP (30%)					
Epidural	97.09	97.87	95.83	96.84	94.16
Intraventricular	100.00	100.00	100.00	100.00	100.00
Intraparenchymal	98.06	88.89	100.00	94.12	93.19
Subdural	99.03	100.00	95.45	97.67	97.10
Subarachnoid	100.00	100.00	100.00	100.00	100.00
Average	**98.83**	**97.35**	**98.26**	**97.73**	**96.89**

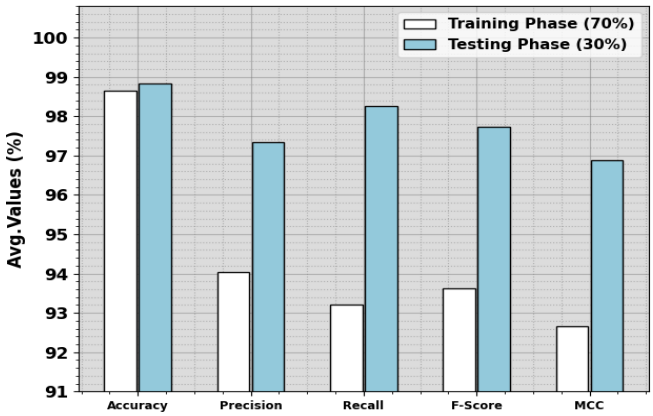

Fig. 4. Average of IEODL-ICHD technique under 70:30 TRAP/TESP

A wide-ranging comparison result of the IEODL-ICHD system on $accu_y$ can be described in Fig. 5 [14]. These attained outcomes denote that the IEODL-ICHD technique gains enriched performance. According to $accu_y$, the IEODL-ICHD method provides increased $accu_y$ of 98.83% although, the PODL-ICHDHM, AIMA-ICHDC, DL-ICH, AMG-LSN, DCNN, SVM, ResNexT, U-Net algorithms get minimized $accu_y$ of 98.43%, 97.13%, 95.64%, 93.41%, 87.86%, 78.24%, 89.19%, and 88%.

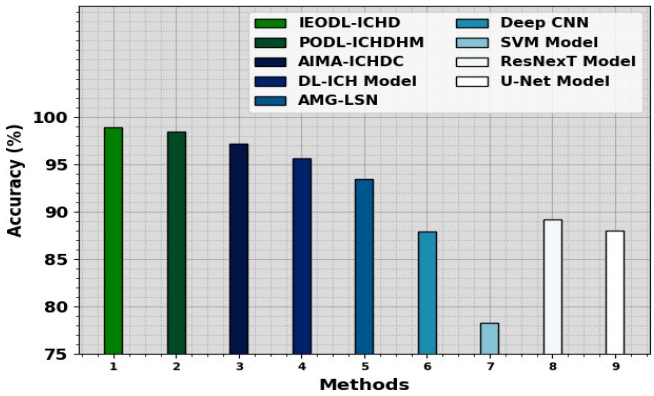

Fig. 5. $Accu_y$ Outcome Of IEODL-ICHD System Compared With Other Algorithms

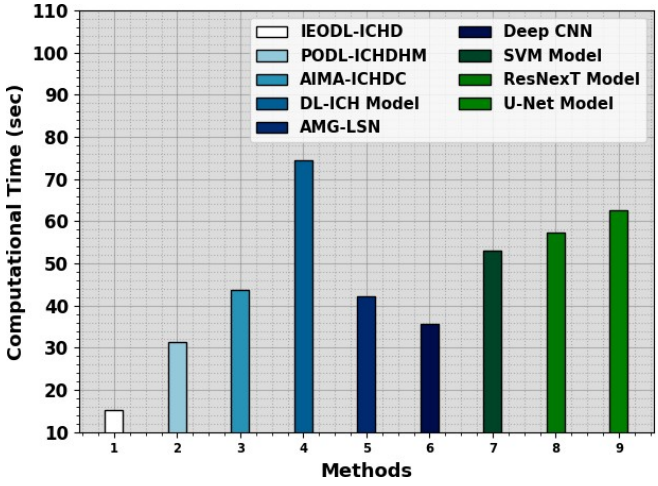

Fig. 6. *CT* Outcome Of IEODL-ICHD System Compared With Other Techniques

An extensive computational time (CT) comparison outcome of the IEODL-ICHD system can be defined in Fig. 6. These accomplished findings signify that the IEODL-ICHD algorithm achieves improved performance. Based on *CT* the IEODL-ICHD technique offers decreased *CT* of 15.16s however, the PODL-ICHDHM, AIMA-ICHDC, DL-ICH, AMG-LSN, DCNN, SVM, ResNexT, U-Net methods acquire diminished *CT* of 31.24s, 43.63s, 74.47s, 42.22s, 35.56s, 53.05s, 57.27s, and 62.52s.

4. Conclusion

In this article, we have presented a novel IEODL-ICHD model on CT images. The main purposes of the IEODL-ICHD methodology encompass four different processes namely UNet segmentation, ResNet18 feature extractor, IEO-based parameter tuning, and XGBoost based classification. The IEODL-ICHD technique starts with the UNet segmentation approach which proficiently outlines the regions of interest for ICH detection. Besides, the IEODL-ICHD technique utilizes a ResNet18 feature extractor to extract high-level features to accurately identify the haemorrhage. Besides, the IEO system is exploited for hyperparameter tuning, safeguarding the model's flexibility to the refined features of the ICH. Lastly, the XGBoost model is applied for accurate recognition and identification of the ICH. The simulation outcomes of the IEODL-ICHD approach are systematically authenticated on CT images, representing greater performance in ICH classification.

REFERENCES

[1] G. Zhang, K. Chen, S. Xu, P. C. Cho, Y. Nan, X. Zhou, C. Lv, C. Li, and G. Xie, ‘‘Lesion synthesis to improve intracranial hemorrhage detection and classification for CT images,’’ Computerized Med. Imag. Graph., vol. 90, Jun. 2021, Art. no. 101929.

[2] M. Karki, J. Cho, E. Lee, M.-H. Hahm, S.-Y. Yoon, M. Kim, J.-Y. Ahn, J. Son, S.-H. Park, K.-H. Kim, and S. Park, ‘‘CT window trainable neural network for improving intracranial hemorrhage detection by combining multiple settings,’’ Artif. Intell. Med., vol. 106, Jun. 2020, Art. no. 101850.

[3] H. Wang, K. Wang, Q. Xue, M. Peng, L. Yin, X. Gu, H. Leng, J. Lu, H. Liu, D. Wang, and J. Xiao, ‘‘Transcranial alternating current stimulation for treating depression: A randomized controlled trial,’’ Brain, vol. 145, no. 1, pp. 83–91, Mar. 2022, doi: 10.1093/brain/awab252.

[4] M. F. Mushtaq, M. Shahroz, A. M. Aseere, H. Shah, R. Majeed, D. Shehzad, and A. Samad, ‘‘BHCNet: Neural network-based brain hemorrhage classification using head CT scan,’’ IEEE Access, vol. 9, pp. 113901–113916, 2021.

[5] M. Ragab, S. M. Alshammari, A. H. Asseri, and W. K. Almutiry, ‘‘Optimal fusion-based handcrafted with deep features for brain cancer classification,’’ Comput., Mater. Continua, vol. 73, no. 1, pp. 801–815, 2022.

[6] J. McLouth, S. Elstrott, Y. Chaibi, S. Quenet, P. D. Chang, D. S. Chow, and J. E. Soun, ‘‘Validation of a deep learning tool in the detection of intracranial hemorrhage and large vessel occlusion,’’ Frontiers Neurol., vol. 12, Apr. 2021, Art. no. 656112.

[7] X. Wang, T. Shen, S. Yang, J. Lan, Y. Xu, M. Wang, J. Zhang, and X. Han, ‘‘A deep learning algorithm for automatic detection and classification of acute intracranial hemorrhages in head CT scans,’’ NeuroImage, Clin., vol. 32, Jan. 2021, Art. no. 102785.

[8] H. Lee, S. Yune, M. Mansouri, M. Kim, S. H. Tajmir, C. E. Guerrier, S. A. Ebert, S. R. Pomerantz, J. M. Romero, S. Kamalian, R. G. Gonzalez, M. H. Lev, and S. Do, ‘‘An explainable deep-learning algorithm for the detection of acute intracranial haemorrhage from small datasets,’’ Nature Biomed. Eng., vol. 3, no. 3, pp. 173–182, Dec. 2018.

[9] S. Lu, J. Yang, B. Yang, Z. Yin, M. Liu, L. Yin, and W. Zheng, ‘‘Analysis and design of surgical instrument localization algorithm,’’ Comput. Model. Eng. Sci., vol. 137, no. 1, pp. 669–685, 2023, doi: 10.32604/cmes.2023.027417.

[10] A. Sage and P. Badura, ‘‘Intracranial hemorrhage detection in head CT using double-branch convolutional neural network, support vector machine, and random forest,’’ Appl. Sci., vol. 10, no. 21, p. 7577, Oct. 2020.

[11] Arman, S.E., Rahman, S.S., Irtisam, N., Deowan, S.A., Islam, M.A., Sakib, S. and Hasan, M., 2023. Intracranial Hemorrhage Classification From CT Scan Using Deep Learning and Bayesian Optimization. *IEEE Access*.

[12] Mansour, R.F. and Aljehane, N.O., 2021. An optimal segmentation with deep learning based inception network model for intracranial hemorrhage diagnosis. *Neural Computing and Applications*, *33*(20), pp.13831-13843.

[13] Alfaer, N.M., Aljohani, H.M., Abdel-Khalek, S., Alghamdi, A.S. and Mansour, R.F., 2022. Fusion-based deep learning with nature-inspired algorithm for intracerebral haemorrhage diagnosis. *Journal of Healthcare Engineering*, *2022*.

[14] Ragab, M., Salama, R., Alotaibi, F.S., Abdushkour, H.A. and Alzahrani, I.R., 2023. Political Optimizer with Deep Learning Based Diagnosis for Intracranial Hemorrhage Detection. *IEEE Access*.

[15] Chen, D., Li, X. and Li, S., 2021. A novel convolutional neural network model based on beetle antennae search optimization algorithm for computerized tomography diagnosis. *IEEE transactions on neural networks and learning systems*.

[16] Phaphuangwittayakul, A., Guo, Y., Ying, F., Dawod, A.Y., Angkurawaranon, S. and Angkurawaranon, C., 2022. An optimal deep learning framework for multi-type hemorrhagic lesions detection and quantification in head CT images for traumatic brain injury. *Applied Intelligence*, pp.1-19.

[17] Saikia, S., Si, T., Deb, D., Bora, K., Mallik, S., Maulik, U. and Zhao, Z., 2023. Lesion detection in women breast’s dynamic contrast-enhanced magnetic resonance imaging using deep learning. *Scientific Reports*, *13*(1), p.22555.

[18] Liu, S., Chen, S., Chen, Z. and Gong, Y., 2023. Fault Diagnosis Strategy Based on BOA-ResNet18 Method for Motor Bearing Signals with Simulated Hydrogen Refueling Station Operating Noise. *Applied Sciences*, *14*(1), p.157.

[19] Yue, L., Hu, P., Chu, S.C. and Pan, J.S., 2023. English Speech Emotion Classification Based on Multi-Objective Differential Evolution. *Applied Sciences*, *13*(22), p.12262.

[20] Mahesh, T.R., Bhardwaj, R., Khan, S.B., Alkhaldi, N., Victor, N. and Verma, A., 2023. An artificial intelligence-based decision support system for early and accurate diagnosis of Parkinson’s Disease. *Decision Analytics Journal*, p.100381.